

Numerical Computation of Space Derivatives by the Complex-Variable-Differentiation Method in the Convolution Quadrature Method Based BEM Formulation

A.I. Abreu¹, W.J. Mansur¹, D. Soares Jr^{1,2} and J.A.M. Carrer³

Abstract: This paper is concerned with the numerical computation of space derivatives of a time-domain (TD-) Boundary Element Method (BEM) formulation for the analysis of scalar wave propagation problems. In the present formulation, the Convolution Quadrature Method (CQM) is adopted, i.e., the basic integral equation of the TD-BEM is numerically substituted by a quadrature formula, whose weights are computed using the Laplace transform of the fundamental solution and a linear multi-step method. In order to numerically compute space derivatives, the present work properly transforms the quadrature weights of the CQM-BEM, adopting the so-called Complex-Variable-Differentiation Method (CVDM). Numerical examples are presented at the end of the paper illustrating the accuracy and potentialities of the proposed formulation.

Keyword: wave propagation, acoustics; boundary element method; convolution quadrature method; complex-variable-differentiation method.

1 Introduction

This work presents an application of the Complex-Variable-Differentiation Method (CVDM) for the numerical computation of space

derivatives in a time-domain (TD-) Boundary Element Method (BEM) formulation for the analysis of scalar wave propagation problems. The CVDM is based on the previous work of Lyness and Moler (1967) and it consists of computing the derivatives of a real variable function by writing this function in terms of its analytic extension to the complex variable plane [Churchill and Brown (1989)].

There are several situations in which an accurate numerical computation of space derivatives is of great importance, considering wave propagation problems, as for instance: (i) calculation of internal fluxes or pressure gradients in acoustic fluids; (ii) evaluation of stress/strain fields taking into account dynamic problems; (iii) calculation of magnetic/electric fields considering electromagnetic wave propagation phenomena, etc. The Finite Difference Method is commonly applied to compute these derivatives, however, the accuracy of this methodology is step-size dependent and usually provides very inaccurate results considering a BEM context. Some important fields where the calculation of derivatives is necessary are, for example, inverse problems (see the works by Huang and Shih (2007), Liu, Liu and Hong (2007), Shiozawa, Kubo, Sakagami and Takagi (2006), Marin, Power, Bowtell, Sanchez, Becker, Glover and Jones (2008) and Mera, Elliott and Ingham (2006)), stability analysis (Ling and Atluri (2006)), topology optimization (as in the recent works by Wang, Lim, Khoo and Wang (2007, 2008)), etc.

One of the advantages of the CVDM is its facility to compute numerical derivatives only taking the imaginary part of the formed complex number. Thus, concerning implementation aspects,

¹ Department of Civil Engineering, COPPE/Federal University of Rio de Janeiro, CP 68506, CEP 21945-970, Rio de Janeiro, RJ, Brazil. Email: anai@coc.ufrj.br, webe@coc.ufrj.br

² Structural Engineering Department, Federal University of Juiz de Fora, Cidade Universitária, CEP 36036-330, Juiz de Fora, MG, Brazil. E-mail: delfim.soares@ufjf.edu.br

³ PPGMNE: Programa de Pós-Graduação em Métodos Numéricos em Engenharia, Universidade Federal do Paraná, CP 19011, CEP 81531-990, Curitiba, PR, Brasil. E-mail: carrer@mat.ufpr.br

basically one just has to convert real variables to complex variables in an existing software code. The use of such a methodology in the present TD-BEM formulation is motivated by the successful results obtained by Gao, Liu and Chen (2002) and Gao and He (2005) in BEM elastoplastic analysis and identification problems (material properties and unknown geometries). Moreover, the CVDM was successfully implemented by Soares Jr, Carrer, Telles and Mansur (2002), for the numerical computation of internal stresses and velocities in an elastodynamic TD-BEM formulation. As it has been highlighted in this work, all the difficulties related to analytically computing space and time derivatives (as for instance, the derivatives of the finite part of the integral) could be avoided by adopting the CVDM.

In the present work, the CVDM is applied to a TD-BEM formulation that employs the Convolution Quadrature Method (CQM) developed by Lubich (1988). In the CQM, the fundamental solution in the Laplace transformed-domain is considered and a numerical approximation of the basic integral equations of the TD-BEM is worked out by a quadrature formula based on a linear multi-step method. The main advantage of the CQM is that it can be applied to problems where the TD fundamental solution is not suitable or else is not available at all. The CQM was firstly applied to scalar wave propagation problems, considering the BEM, in the work of Abreu, Carrer and Mansur (2003); this formulation is denoted here as CQM-BEM. The CQM has already been employed successfully in many other works, considering different physical problems: Schanz and Antes (1997), Gaul and Schanz (1999), Schanz (2001) and Schanz, Antes and Rüberg (2005) applied the CQM to (poro/visco-) elastodynamic BEM analyses. Application of the CQM to plane frame dynamic modelling was performed by Antes, Schanz and Alvermann (2004). A method based on Duhamel integrals, in combination with the CQM, for the analysis of one-dimensional wave propagation in a layered medium was presented by Moser, Antes and Beer (2005), which was extended to plane strain elastodynamic BEM-FEM (-Finite Element

Method) coupling later [Moser, Antes and Beer (2005)]. All the BEM formulations mentioned so far do not consider initial conditions; in a recent work of Abreu, Mansur and Carrer (2006), a numerical technique was presented in order to consider non-null initial conditions in a CQM-BEM context.

At the end of the paper numerical examples demonstrate that the CVDM is appropriate for computing space derivatives of wave propagation problems in a CQM based BEM.

2 The Convolution Quadrature Method applied to the BEM

The scalar wave equation is written as [Morse and Feshbach (1953)]:

$$\nabla^2 u(X,t) - \frac{1}{c^2} \frac{\partial^2 u(X,t)}{\partial t^2} = 0 \quad (1)$$

where $u(X,t)$ represents the 2D potential, t and X stand for time and space coordinates, respectively, and c is the wave propagation velocity. The boundary conditions are given by:

$$u(X,t) = \bar{u}(X,t) \quad X \in \Gamma_u \quad (2)$$

$$p(X,t) = \frac{\partial u(X,t)}{\partial n} = \bar{p}(X,t) \quad X \in \Gamma_p \quad (3)$$

In the above expressions, $\partial u(X,t)/\partial n$ represents the flux and $\Gamma = \Gamma_u \cup \Gamma_p$ stands for the boundary of a domain Ω . The basic time-domain integral equation, which corresponds to the scalar wave propagation problem (Eq. (1)) with null initial conditions (i.e., $u(X,0) = 0$ and $\partial u(X,0)/\partial t = 0$ in $X \in \Omega \cup \Gamma$), is written as [Mansur (1983), Mansur and Carrer (1993), Dominguez (1993)]:

$$c(\xi)u(\xi,t) = \int_{\Gamma} \int_0^{t^+} u^*(X,t;\xi,\tau)p(X,\tau)d\tau d\Gamma - \int_{\Gamma} \int_0^{t^+} p^*(X,t;\xi,\tau)u(X,\tau)d\tau d\Gamma \quad (4)$$

where $c(\xi)$ is a geometrical coefficient and $u^*(X,t;\xi,\tau)$ is the fundamental solution representing the effect, at a field point X , at time t , due to an impulsive source applied at time

τ , at a source point ξ . In the same equation, $p^*(X, t; \xi, \tau) = \partial u^*(X, t; \xi, \tau) / \partial n$.

Considering the CQM, the discretized version of Eq. (4), for each source point ξ_i , is written as [Abreu, Carrer and Mansur (2003)]:

$$c(\xi_i)u(\xi_i, t_n) = \sum_{j=1}^J \sum_{k=0}^n \mathbf{g}_{n-k}^j(\xi_i, \Delta t) \mathbf{p}_k^j - \sum_{j=1}^J \sum_{k=0}^n \mathbf{h}_{n-k}^j(\xi_i, \Delta t) \mathbf{u}_k^j \quad (5)$$

where J is the number of elements Γ_j used to approximate the boundary ($j = 1, 2, \dots, J$), Δt is the time-step interval ($t_n = n\Delta t$ for $n = 0, 1, 2, \dots, NT$, where NT is the total number of time sampling). The nodal values \mathbf{p}_k^j and \mathbf{u}_k^j are given by:

$$\mathbf{p}_k^j = \mathbf{p}^j(k\Delta t) \text{ and } \mathbf{u}_k^j = \mathbf{u}^j(k\Delta t) \quad (6)$$

The quadrature weights \mathbf{g}_n and \mathbf{h}_n in Eq. (5) are computed by the following expressions (where $s = \gamma(z)/\Delta t$):

$$\mathbf{g}_n^j(\xi_i, \Delta t) = \frac{1}{2\pi i} \int_{\Gamma_j} \left(\int_{C_\rho} \hat{u}^*(r, s) z^{-n-1} dz \right) \Phi^j(X) d\Gamma, \quad (7)$$

$$\mathbf{h}_n^j(\xi_i, \Delta t) = \frac{1}{2\pi i} \int_{\Gamma_j} \left(\int_{C_\rho} \hat{p}^*(r, s) z^{-n-1} dz \right) \Phi^j(X) d\Gamma, \quad (8)$$

where $r = |X - \xi_i|$ represents the distance between the source and field points. The quadrature weights \mathbf{g}_n and \mathbf{h}_n represent, respectively, the coefficients of the power series in which $\hat{u}^*(r, s)$ and $\hat{p}^*(r, s)$ are developed. These coefficients are determined by the Cauchy's integral formula, C_ρ is the contour employed to perform the integration given by $|z| = \rho$, where ρ is the radius of a circle in the domain of analyticity of $\hat{u}^*(r, s)$. Usually, the inner integrals in Eq. (7) and (8) are numerically determined. Thus, expressions (7) and (8), after a polar coordinate transformation, can be approximated by a trapezoidal rule as indicated be-

low:

$$\mathbf{g}_n^j(\xi_i, \Delta t) = \frac{\rho^{-n}}{L} \sum_{l=0}^{L-1} \int_{\Gamma_j} \hat{u}^*(r, s_l) \Phi^j(X) d\Gamma e^{-inl2\pi/L}, \quad (9)$$

$$\mathbf{h}_n^j(\xi_i, \Delta t) = \frac{\rho^{-n}}{L} \sum_{l=0}^{L-1} \int_{\Gamma_j} \hat{p}^*(r, s_l) \Phi^j(X) d\Gamma e^{-inl2\pi/L}, \quad (10)$$

In the above expressions, $\Phi^j(X)$ represents the interpolation functions employed in the boundary discretization and $s_l = \gamma(\rho e^{il2\pi/L})/\Delta t$. In expressions (7) and (9), $\hat{u}^*(r, s)$ is the Laplace transform of the fundamental solution $u^*(r, t)$. In expressions (8) and (10), $\hat{p}^*(r, s)$ is the Laplace transform of $p^*(r, t)$.

The fundamental solution $\hat{u}^*(r, s)$ and its normal derivative are given by [Morse and Feshbach (1953)]:

$$\hat{u}^*(r, s) = 2K_0(sr) \quad (11)$$

and

$$\hat{p}^*(r, s) = \frac{\partial \hat{u}^*(r, s)}{\partial r} \frac{\partial r}{\partial n} = -2SK_1(sr) \frac{\partial r}{\partial n} \quad (12)$$

where $K_0(sr)$ is the modified Bessel function of order zero and second type and $K_1(sr)$ is the modified Bessel function of first order and second type [Abramowitz and Stegun (1984)].

The function γ , used in Eqs. (7) to (10), is the quotient of the characteristic polynomials generated by a linear multi-step method. When $u^*(r, s)$ in Eq. (9) (or $p^*(r, s)$ in Eq. (10)) is computed with an error ε , the choice of $L = NT$ and $\rho^{NT} = \sqrt{\varepsilon}$ produces an error of order $O\sqrt{\varepsilon}$ in $\mathbf{g}_n^j(r, \Delta t)$ (or in $\mathbf{h}_n^j(r, \Delta t)$) [Lubich (1988)].

Note that, in the computation of the integration weights by means of either the formula (9) or (10), there are two parameters, L and ε , influencing the accuracy of the solution. These parameters must be chosen carefully in order to reach good results. Theoretically ρ represents the radius of a circle C_ρ in the domain of analyticity of the function $\hat{u}(s)$, and this circle is the integration path around the singularity $z = 0$ of the Cauchy's integration formula (see Eqs. (7)-(8)). Values for the radius

ρ can be calculated from different values of ε : when ε is small, values for ρ become very small, and consequently it results in a loss of accuracy of the numerical integration due to the approximation introduced by the trapezoidal rule. The influence of ρ was numerically studied and, after some numerical tests, the authors were led to the value of the parameter $\varepsilon = 10^{-4}$ as the best choice for this kind of problem; the analysis leading to this conclusion can be found in Abreu, Mansur and Carrer (2006).

Equation (5) can be rewritten in matrix notation as follows:

$$\mathbf{C}\mathbf{u}^n = \sum_{k=0}^n \mathbf{G}^{n-k} \mathbf{p}^k - \sum_{k=0}^n \mathbf{H}^{n-k} \mathbf{u}^k \quad (13)$$

where \mathbf{C} is a diagonal matrix that contains the coefficients $c(\xi_i)$, \mathbf{G} and \mathbf{H} are the final boundary element influence matrices and n and k correspond to the discrete times $t_n = n\Delta t$ and $t_k = k\Delta t$, respectively. After imposing boundary conditions, Eq. (13) reads:

$$\mathbf{A}^0 \mathbf{y}^n = \mathbf{f}^n + \sum_{k=0}^{n-1} \mathbf{f}^k \quad (14)$$

where vector \mathbf{f}^k previous time contributions are accounted for, as follows:

$$\mathbf{f}^k = \mathbf{G}^{n-k} \mathbf{p}^k - \mathbf{H}^{n-k} \mathbf{u}^k \quad (15)$$

In expression (14), the unknowns and the contributions of prescribed boundary conditions at time $t_n = n\Delta t$ are stored, respectively, in vectors \mathbf{y}^n and \mathbf{f}^n .

A deeper discussion about the general CQM formulation can found in [Lubich (1988)]; for a more detailed discussion concerning the CQM-BEM applied to the scalar wave equation see Abreu, Carrer and Mansur (2003).

3 Space derivatives

The numerical procedure employed in this work for the computation of space derivatives is based on the CVDM and is derived from the earlier work of Lyness and Moler (1967). In this procedure,

the real valued function $f(x)$ must have an analytic extension to the complex plane (to avoid conflict in the notation, this extension will be identified with the same symbol f). In the usual complex notation, the function f can be expressed as $f(z) = u(x, y) + iv(x, y)$, where $z = x + iy$; u and v are real functions of real arguments x and y and i stands for the imaginary unit. As f is an analytic function, the Cauchy-Reimann conditions:

$$\frac{\partial u}{\partial x} = \frac{\partial v}{\partial y} \text{ and } \frac{\partial u}{\partial y} = -\frac{\partial v}{\partial x} \quad (16)$$

are valid and the complex derivative of f is calculated as [Churchill and Brown (1989)]:

$$\frac{df}{dz}(z) = -i \frac{\partial u}{\partial y} + \frac{\partial v}{\partial y} \quad (17)$$

As f is an analytic extension of a real valued function, v and its partial derivative with respect to x vanish when $y = 0$, i.e., $v(x, 0) = 0$ and $\partial v(x, 0)/\partial x = 0$. It therefore follows by Eq. (16) that $\partial u(x, 0)/\partial y = 0$. Then, by Eq. (17):

$$\begin{aligned} \frac{df}{dz}(x) &= \frac{\partial v(x, 0)}{\partial y} \approx \lim_{\Delta \rightarrow 0} \frac{v(x, 0 + \Delta) - v(x, 0)}{\Delta} \\ &= \lim_{\Delta \rightarrow 0} \frac{v(x, \Delta)}{\Delta} = \lim_{\Delta \rightarrow 0} \frac{\text{Im}f(x + i\Delta)}{\Delta} \end{aligned} \quad (18)$$

where the symbol Im represents the imaginary part of the function. Finally, Eq. (18) can be approximated for a small enough real value Δ , as follows:

$$\frac{df}{dz}(x) \approx \frac{\text{Im}f(x + i\Delta)}{\Delta} \quad (19)$$

From Eq. (19) it is possible to compute the first derivative of f without producing cancellation errors (that is the case when finite difference techniques are applied). In the works of Gao, Liu and Chen (2002), Gao and He (2005) and Soares Jr, Carrer, Telles and Mansur (2002), it is shown that Eq. (19) becomes very accurate, even when Δ is a very small quantity.

4 The CVDM applied to the CQM-BEM

In order to compute space derivatives at interior points using the CVDM, Eq. (19) is applied to the

function u . If $\xi_i = (\xi_x, \xi_y)$, the partial derivative of u with respect to ξ_x reads:

$$\frac{\partial u}{\partial \xi_x}(\xi_i) \approx \frac{\text{Im}u(\xi_x + i\Delta, \xi_y)}{\Delta} \quad (20)$$

From Eq. (5) $c(\xi_i) = S$ for interior points), defining $\xi_{ix} = (\xi_x + i\Delta, \xi_y)$, and introducing $\frac{1}{\Delta}\text{Im}[\cdot]$ into the sums, the numerical space derivative with respects to ξ_x of the potential $u(\xi_i, t_n)$ is computed as:

$$\begin{aligned} \frac{\partial u}{\partial \xi_x}(\xi_i, t_n) &\approx \sum_{j=1}^J \sum_{k=0}^n \frac{1}{\Delta} \text{Im} \left[\mathbf{g}_{n-k}^j(\xi_{ix}, \Delta t) \right] \mathbf{p}_k^j \\ &\quad - \sum_{j=1}^J \sum_{k=0}^n \frac{1}{\Delta} \text{Im} \left[\mathbf{h}_{n-k}^j(\xi_{ix}, \Delta t) \right] \mathbf{u}_k^j \end{aligned} \quad (21)$$

Equation (21) shows that the new quadrature weights are the derivatives of the original weights \mathbf{g}_n and \mathbf{h}_n computed using the CVDM. The weights can be obtained in an efficient way by the Fast Fourier Transform (FFT) algorithm [Cooley and Tukey (1965); Brigham (1974)]:

$$\mathbf{g}_n^j(\xi_{ix}, \Delta t) = \frac{\rho^{-n}}{L} \int_{\Gamma_j} \hat{\mathbf{U}}^*(r, n) \Phi^j(X) d\Gamma \quad (22)$$

$$\mathbf{h}_n^j(\xi_{ix}, \Delta t) = \frac{\rho^{-n}}{L} \int_{\Gamma_j} \hat{\mathbf{P}}^*(r, n) \Phi^j(X) d\Gamma \quad (23)$$

where $\hat{\mathbf{U}}^*(r, \cdot)$ and $\hat{\mathbf{P}}^*(r, \cdot)$ are the FFT transforms of vectors $\hat{\mathbf{u}}^*(r, \mathbf{S})$ and $\hat{\mathbf{p}}^*(r, \mathbf{S})$, respectively, and \mathbf{S} is the vector $(s_0, s_1, \dots, s_{L-1})$. Note that, if the Gauss quadrature formula is applied to the integrals of Eqs. (22)-(23), one has to call the FFT routine once for each Gauss point. The integration on the element can be performed before the FFT in order to reduce the number of times that the FFT routine is used.

In order to calculate the space derivatives of the potential function using Eqs. (21), (22) and (23), the original codes of the CQM-BEM need to undergo two main modifications:

I) All the variables declared of real type that become complex by reason of the imaginary increment, must be declared of complex type,

II) The ‘real’ and ‘imaginary’ parts of vectors $\hat{\mathbf{u}}^*(r, \mathbf{S})$ and $\hat{\mathbf{p}}^*(r, \mathbf{S})$, and all intermediary calculations derived from \mathbf{S} must be stored separately.

The vector \mathbf{V} is obtained by mean of $\mathbf{V} = \mathbf{V}_R + \mathbf{V}_I$, where \mathbf{V}_R and \mathbf{V}_I are complex vectors such as $\text{FFT}(\mathbf{V}_R)$ is a real vector and $\text{FFT}(\mathbf{V}_I)$ is pure imaginary. All calculations must be done in such a way that the floating-point representation error of the ‘real’ parts does not affect the accuracy of the ‘imaginary’ parts.

Note that item II is required as the original CQM-BEM code already employs complex arithmetic. For $\Delta = 0$ all ‘imaginary’ parts are null. For positive values of Δ the significant information about the perturbation corresponds to the ‘imaginary’ parts of the vectors and must be stored separately. These ‘imaginary’ parts are tiny for $\Delta \ll 1$ and can also be smaller than the absolute errors of the ‘real’ parts, so they have to be stored separately in order to preserve that information. From the computational point of view, the storage of ‘real’ and ‘imaginary’ parts duplicates the memory requirement. However, since the FFT transform of these vectors is pure real or pure imaginary, only half of the coefficients must be actually stored [Brigham (1974)].

One difficulty arises in the implementation of item II: in the CQM-BEM code some transcendental functions (the Bessel functions and its derivatives) are present. These functions are non-linear, therefore the ‘real’ and ‘imaginary’ parts of the function value cannot be obtained independently from the ‘real’ and ‘imaginary’ parts of the argument [Amos (1995)]. However, these functions can be linearized by truncating the Taylor’s series expanded around the ‘real’ part of the complex argument. As the CVDM employs very small values for Δ , the error due to this approximation is negligible. For example, if $\mathbf{W} = \mathbf{W}_R + \mathbf{W}_I$ is the argument of the Bessel functions $K_{0,1}$:

$$\begin{aligned} \mathbf{V} &= K_{0,1}(\mathbf{W}_R + \mathbf{W}_I) \\ &\approx K_{0,1}(\mathbf{W}_R) + K'_{0,1}(\mathbf{W}_R) \mathbf{W}_I \end{aligned} \quad (24)$$

thus,

$$\mathbf{V}_R \approx K_{0,1}(\mathbf{W}_R) \text{ and } \mathbf{V}_I \approx K'_{0,1}(\mathbf{W}_R) \mathbf{W}_I \quad (25)$$

where

$$\begin{aligned} K'_{0,1}(x) &= -K_1(x) \text{ and} \\ K'_1(x) &= K_0(x) + \frac{1}{x} K_1(x) \end{aligned} \quad (26)$$

Consider, for example, the following pseudo-code corresponding to the original code for obtaining $\hat{\mathbf{U}}^*(r, \cdot)$:

Data: Gauss coordinate η , Source point ξ_i , Vector \mathbf{S}

Calculate:

- i. $X = X(\eta)$
- ii. $r = |X - \xi_i|$
- iii. $\mathbf{W} = \mathbf{S}r$
- iv. $\mathbf{V} = K_0(\mathbf{W})$
- v. $\hat{\mathbf{u}}^* = 2\mathbf{V}$
- vi. $\hat{\mathbf{U}}^* = \text{FFT}(\hat{\mathbf{u}}^*)$

Note that \mathbf{S} is the inverse Fourier transform of a real vector. In fact, since $s_l = \gamma(\rho e^{il2\pi/L})/\Delta t$ and the polynomial $\gamma(z)$ of order p is generated from $\gamma(z) = \sum_{n=1}^p \frac{1}{n}(1-z)^n$ [see Lubich (1988)], s_l can be written as:

$$\begin{aligned} s_l &= \frac{1}{\Delta t} \sum_{n=1}^p \frac{1}{n} \left(1 - \rho e^{il2\pi/L}\right)^n \\ &= \frac{1}{\Delta t} \sum_{n=1}^p \frac{1}{n} \sum_{j=0}^n \binom{n}{j} (-\rho)^j e^{ilj2\pi/L} \\ &= \frac{1}{L} \sum_{j=0}^p \frac{L}{\Delta t} (-\rho)^j \sum_{n=\max(i,j)}^p \frac{1}{n} \binom{n}{j} e^{ilj2\pi/L} \end{aligned} \quad (27)$$

Consequently, the vector \mathbf{S} is the inverse Fourier transform of the real vector (d_1, \dots, d_L) given by:

$$d_j = \frac{L}{\Delta t} (-\rho)^j \sum_{n=\max(i,j)}^p \frac{1}{n} \binom{n}{j} \quad (28)$$

Thus, $\mathbf{S}_R = \mathbf{S}$ and $\mathbf{S}_I = 0$.

The pseudo-code corresponding to the implementation of the CVDM considering the item II is given by:

Data: Gauss coordinate η , Source point ξ_{ix} , Vector \mathbf{S} ($= \mathbf{S}_R$)

Calculate:

- i. $X = X(\eta)$
- ii. $r = |X - \xi_{ix}|$

iii. $\mathbf{W}_R = \mathbf{S}r$ and $\mathbf{W}_I = i\mathbf{S}Im(r)$

iv. $\mathbf{V}_R = K_0(\mathbf{W}_R)$ and $\mathbf{V}_I = K'_0(\mathbf{W}_R)\mathbf{W}_I$

v. $\hat{\mathbf{u}}^* = 2\mathbf{V}_I$

vi. $\hat{\mathbf{U}}^* = \text{FFT}(\hat{\mathbf{u}}^*)$

Note that at point v the ‘real’ part of $\hat{\mathbf{u}}^*$ was abandoned since only the imaginary part of \mathbf{g}_n is relevant.

5 Examples

In order to verify the accuracy of the proposed methodology, numerical results are presented next. The dimensionless parameter $\beta = c\Delta t/l$ is adopted here to estimate the time-step length employed in the analyses (l is the smallest boundary element length). In all the following examples, the wave propagation velocity is given by $c = 1$.

The methodology proposed by the present work is referred by CVDM-CQM-BEM ($L = NT$, $\varepsilon = 10^{-4}$ and $\Delta = 10^{-10}$ have been adopted and the function $\gamma(z)$ was taken as the second order polynomial function). In the following sub-sections, some results are compared with those related to the standard TD-BEM formulation. When the CVDM is applied to the TD-BEM, this technique is referred here as CVDM-TD-BEM.

5.1 One-dimensional rod under a Heaviside-type forcing function

This example consists of a one-dimensional like rod, fixed at $x = a$, with free-end boundary condition at $x = 0$ (see Fig. 1). At the boundary $x = 0$ and at time $t = 0$ a Heaviside-type forcing function is applied, as indicated by: $p(0, t) = (P/E)H(t, 0)$, where $P/E = 1$ and E is the longitudinal elasticity modulus. The boundary element mesh adopted is composed of 24 linear elements and the numerical results are computed at the interior point $A(a/2, 0)$.

Three different approaches are compared:

FD: this implementation corresponds to the classic Finite Differences procedure.

CVDM-1: complex variable approach that just declares double complex the original variables of real double precision type (Item I of Section 4).

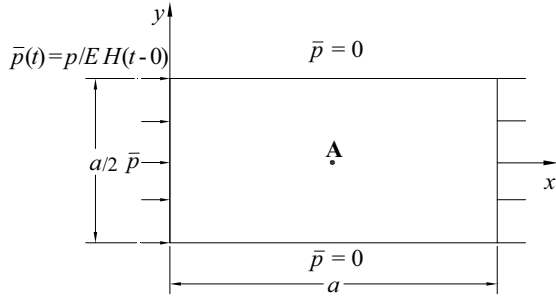


Figure 1: One-dimensional rod: geometry and boundary conditions.

CVDM-2: complex variable approach that declares the variables as double complex and stores the ‘real’ and ‘imaginary’ parts separately (Items I and II of Section 4).

The error $Er(\Delta) = \frac{|u^{ref} - u^{num}(\Delta)|}{u_{max}^{ref}}$ is adopted to compare the accuracy of the implementations, where u^{ref} is a reference value obtained after analytic differentiation of the boundary equation and integration on the same mesh, and $u^{num}(\Delta)$ corresponds to the numerical result obtained using one of the numerical approaches, i.e., FD, CVDM-1 or CVDM-2.

Figure 2 shows the errors of the space derivative calculated at point A for a fixed time $ct/a = 6.0$ and for different values of the step-size increment Δ .

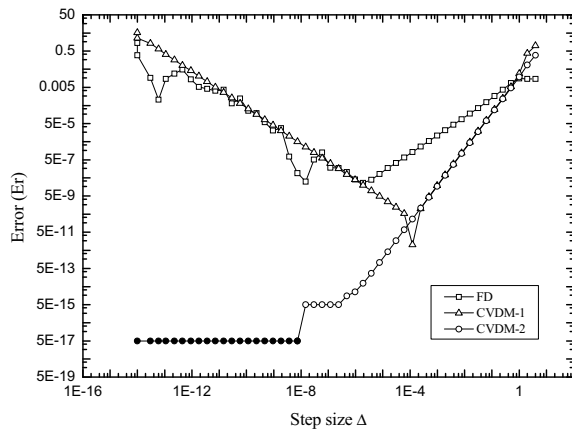


Figure 2: Errors of the calculated space derivative of example 5.1 using the FD and the CVDM approaches. Solid circles: machine precision.

As it can be seen in Fig. 2, the error of the FD approximation is in agreement with the theoretic $O(\Delta)$ behavior for large increments and like $O(1/\Delta)$ for small ones due to the cancellation errors. The error of the CVDM-1 approach presents a higher order behavior for large increments but is similarly affected by the cancellation errors for small values of Δ . The behavior of the CVDM-2 error for small values of Δ is quite different than the FD or the CVDM-1 errors: it becomes stable and seems not to be affected by the cancellation errors. Further, for Δ less than $1.0e-8$ the numerical result matches exactly the reference value, and is indicated in Fig. 2 by the solid circles (as the zero value is out of range in the logarithmic scale, the machine precision is plotted instead of the real error and indicated by solid circles symbols).

The potential space derivative ($\partial u / \partial x$) time-history at interior point A obtained with the appropriated CVDM-CQM-BEM (i.e., the CVDM-2 implementation) with $\beta = 0.6$ ($\Delta t = 0.6$) is presented in Fig. 3.

The results are compared, in the same figure, with the 1D analytical answer [Graff (1975)] and with the CVDM-TD-BEM formulation, for $\beta = 0.6$ ($\Delta t = 0.6$). As one can observe, the proposed formulation gives accurate results.

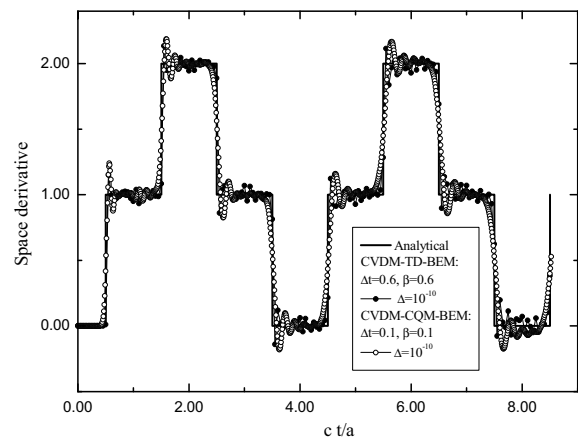


Figure 3: Numerical space derivatives ($\partial u / \partial x$) at point A for the one-dimensional rod.

5.2 Circular cavity under a Heaviside-type forcing function

This second example consists of a circular cavity of radius R submitted to an internal pressure applied at $t = 0$ and kept constant from this time onwards. A sketch of the model is presented in Fig. 4. The adopted boundary element mesh is composed of 24 linear elements, the point $B(2R, 0)$ being where the responses are calculated.

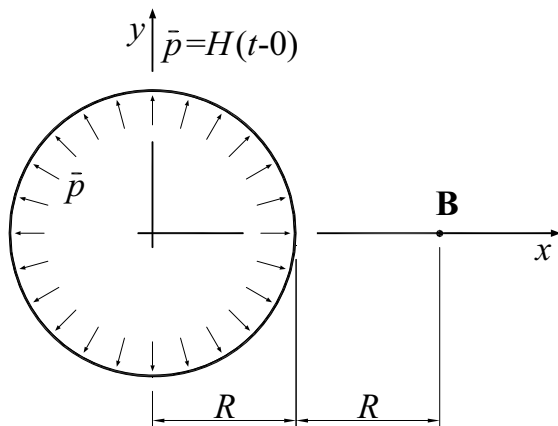


Figure 4: Circular cavity: geometry and boundary conditions.

Figure 5 shows the errors of the space derivative calculated at point B for a fixed time $ct/a = 2.0$ and for different values of the step-size increment Δ .

As can it be seen in Fig. 5, the error graphs for this example is similar to that of example 5.1. Again, the CVDM-2 has the best performance presenting negligible errors when the increment Δ is less than $1.0e-8$.

The results obtained by the appropriated CVDM-CQM-BEM (i.e., the CVDM-2 implementation) are depicted in Fig. 6 and they are, once again, in good agreement with those provided by the CVDM-TD-BEM.

As it can be noticed (Figs. 3 and 6), both BEM formulations present typical numerical oscillations around the discontinuities of the space derivative.

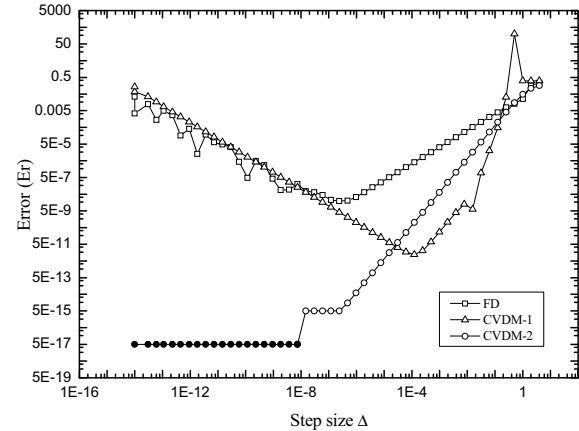


Figure 5: Errors of the calculated space derivative of example 5.2 using the FD and the CVDM approaches. Solid circles: machine precision.

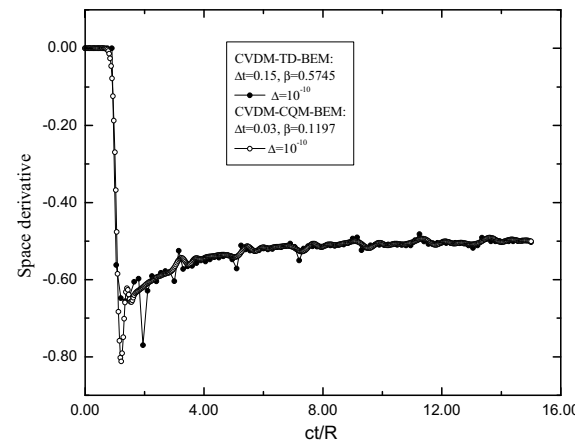


Figure 6: Numerical space derivatives ($\partial u/\partial x$) at point B for the circular cavity.

6 Conclusions

In the present work, a formulation that computes numerical space derivatives by means of the Complex-Variable-Differentiation Method was implemented on a Convolution Quadrature Method based BEM formulation. The CQM-BEM uses a complex fundamental solution to solve scalar wave propagation problem.

The CVDM has been applied, until now, to compute numerically derivatives of real functions. These real functions have to be calculated by a computer code that employs real arithmetic.

In this work, the CVDM is successfully extended

to the case of CQM-BEM codes that employ complex arithmetic. The proposed approach is based on storing separately the ‘real’ and ‘imaginary’ parts of the complex variables and linearization of nonlinear functions. Two examples were solved showing that for small size of the increment the proposed approach is much more accurate than the Finite Difference or the classic Complex-Variable-Differentiation Methods.

Acknowledgement: This work was developed under the financial support of the Brazilian Research Councils CNPq (Conselho Nacional de Desenvolvimento Científico e Tecnológico) and FAPERJ (Fundação de Amparo à Pesquisa do Estado do Rio de Janeiro): the first author is supported by the Grants nos. 150805/2003-9 and 502560/2003-7 of the CNPq and no. E-26/100.904/2007 of the FAPERJ.

References:

- Abramowitz, M.; Stegun, I. A.** (1984): *Handbook of mathematical functions*, Dover Publications, New York.
- Abreu, A. I.; Carrer, J. A. M.; Mansur, W. J.** (2003): Scalar wave propagation in 2d: a BEM formulation based on the operational quadrature method, *Engineering Analysis with Boundary Elements*, vol. 27, pp. 101-105.
- Abreu, A. I.; Mansur, W. J.; Carrer, J. A. M.** (2006): Initial conditions contribution in a BEM formulation based on the operational quadrature method, *International Journal for Numerical Methods in Engineering*, vol. 67 (3), pp. 417-434.
- Antes, H.; Schanz, M.; Alvermann, S.** (2004): Dynamic analyses of plane frames by integral equations for bars and Timoshenko beams, *Journal of Sound and Vibration*, vol. 276, pp. 807-836.
- Amos, D. E.** (1995): A remark on algorithm 644: a portable package for Bessel functions of a complex argument and nonnegative order, *ACM Transactions on Mathematical Software*, vol. 21 (4), pp. 388-393.
- Brigham, E. O.** (1974): *The fast Fourier transform*, Prentice-Hall, Inc., New York.
- Churchill, R. V.; Brown, J. W.** (1989): *Complex Variables and Applications*, McGraw-Hill (4th ed.), New York.
- Cooley, J. W.; Tukey, J. W.** (1965): An algorithm for the machine calculation of complex Fourier series, *Math. Comput.*, vol. 19, pp. 297-301.
- Dominguez, J.** (1993): Boundary elements in dynamics, *Computational Mechanics Publications*, Southampton and Boston.
- Gao, X. W.; Liu, D. D.; Chen, P. C.** (2002): Computation of internal stresses in nonlinear BEM using a numerically-exact complex-variable approach, *Electronic Journal of Boundary Elements* (vol. BETEQ 2001), vol. 3, pp. 303-310.
- Gao, X. W.; Liu, D. D.; Chen, P. C.** (2002): Internal stresses in inelastic BEM using complex-variable differentiation, *Computational Mechanics*, vol. 28, pp. 40-46.
- Gao, X. W.; He, M. C.** (2005): A new inverse analysis approach for multi-region heat conduction BEM using complex-variable-differentiation method, *Engineering Analysis with Boundary Elements*, vol. 29, pp. 788-795.
- Gaul, L.; Schanz, M.** (1999): A comparative study of three boundary element approaches to calculate the transient response of viscoelastic solids with unbounded domains, *Computer Methods in Applied Mechanics and Engineering*, vol. 179, pp. 111-123.
- Graff, K. F.** (1975): *Wave motion in elastic solids*, Dover Publications, New York.
- Huang, C.-H.; Shih, C.-C.** (2007): An inverse problem in estimating simultaneously the time dependent applied force and moment of an Euler-Bernoulli beam. *CMES: Computer Modeling in Engineering and Sciences*, vol. 21, pp. 239-254.
- Ling, X.; Atluri, S. N.** (2006): Stability analysis for inverse heat conduction problems. *CMES: Computer Modeling in Engineering and Sciences*, vol. 13, pp. 219-228.
- Liu, C.-S.; Liu, L.-W.; Hong, H.-K.** (2007): Highly accurate computation of spatial-dependent heat conductivity and heat capacity in inverse thermal problem. *CMES: Computer Modeling in Engineering and Sciences*, vol. 17, pp. 1-18.

- Lubich, C.** (1988): Convolution quadrature and discretized operational calculus I, *Numerische Mathematik*, vol. 52, pp. 129-145.
- Lubich, C.** (1988): Convolution quadrature and discretized operational calculus II, *Numerische Mathematik*, vol. 52, pp. 413-425.
- Lyness, J. N.; Moler, C. B.** (1967): Numerical differentiation of analytic functions, *Journal of Numerical Analysis*, vol. 4, pp. 202-210.
- Mansur, W. J.** (1983): A time-stepping technique to solve wave propagation problems using the boundary element method, *PhD Thesis*, University of Southampton, UK.
- Mansur, W. J.; Carrer, J. A. M.** (1993): Two dimensional transient BEM analysis for the wave equation: kernels, *Engineering Analysis with Boundary Elements*, vol. 12, pp. 283-288.
- Mansur, W. J.; Abreu, A. I.; Carrer, J. A. M.** (2004): Initial conditions contribution in frequency-domain BEM analysis, *CMES: Computer Modeling in Engineering and Sciences*, vol. 6 (1), pp. 31-42.
- Mansur, W. J.; Soares Jr, D.; Ferro, M. A. C.** (2004): Initial conditions in frequency domain analysis: the FEM applied to the scalar wave equation, *Journal of Sound and Vibration*, vol. 270, pp. 767-780.
- Marin, L.; Power, H.; Bowtell, R.W.; Sanchez, C. C.; Becker, A. A.; Glover, P.; Jones, A.** (2008): Boundary element method for an inverse problem in magnetic resonance imaging gradient coils. *CMES: Computer Modeling in Engineering and Sciences*, vol. 23, pp. 149-174.
- Mera, N. S.; Elliott, L.; Ingham, D. B.** (2006): The detection of super-elliptical inclusions in infrared computerized axial tomography. *CMES: Computer Modeling in Engineering and Sciences*, vol. 15, pp. 107-114.
- Morse, P. M.; Feshbach, H.** (1953): *Methods of theoretical physics*, McGraw-Hill, New York.
- Moser, W.; Antes, H.; Beer, G.** (2005): A Duhamel integral based approach to one-dimensional wave propagation analysis in layered media, *Computational Mechanics*, vol. 35, pp. 115-126.
- Moser, W.; Antes, H.; Beer, G.** (2005): Soil-structure interaction and wave propagation problems in 2D by a Duhamel integral based approach and the convolution quadrature method, *Computational Mechanics*, vol. 36 (6), pp. 431-443.
- Schanz, M.; Antes, H.** (1997): A new visco- and elastodynamic time domain boundary element formulation, *Computational Mechanics*, vol. 20, pp. 452-459.
- Schanz, M.; Antes, H.** (1997): Application of 'operational quadrature methods' in time domain boundary element methods, *Meccanica*, vol. 32, pp. 179-186.
- Schanz, M.** (2001): Application of 3D time domain boundary element formulation to wave propagation in poroelastic solids, *Engineering Analysis with Boundary Elements*, vol. 25, pp. 363-376.
- Schanz, M.** (2001): Wave propagation in viscoelastic and poroelastic continua: a boundary element approach, Springer, Berlin, New York.
- Schanz, M.; Antes, H.; Rüberg, T.** (2005): Convolution quadrature boundary element method for quasi-static visco- and poroelastic continua, *Computers and Structures*, vol. 83, pp. 673-684.
- Shiozawa, D.; Kubo, S.; Sakagami, T.; Takagi, M.** (2006): Passive electric potential CT method using piezoelectric material for identification of plural cracks. *CMES: Computer Modeling in Engineering and Sciences*, vol. 11, pp. 27-36.
- Soares Jr, D.; Carrer, J. A. M.; Telles, J. C. F.; Mansur, W. J.** (2002): Numerical computation of internal stress and velocity in time-domain BEM formulation for elastodynamics, *Computational Mechanics*, vol. 30, pp. 38-47.
- Wang, S.Y.; Lim, K.M.; Khoo, B.C.; Wang, M.Y.** (2007): On Hole Nucleation in Topology Optimization Using the Level Set Methods. *CMES: Computer Modeling in Engineering and Sciences*, vol.21, no.3, pp.219-237.
- Wang, S.Y.; Lim, K.M.; Khoo, B.C.; Wang, M.Y.** (2008): A Hybrid Sensitivity Filtering Method for Topology Optimization. *CMES: Computer Modeling in Engineering and Sciences*, vol.24, no.1, pp.21-50.